

# Electrically detected magnetic resonance using radio-frequency reflectometry

H. Huebl,<sup>\*</sup> R. P. Starrett, D. R. McCamey,<sup>†</sup> A. J. Ferguson,<sup>‡</sup> and L. H. Willems van Beveren

*Australian Research Council Centre of Excellence for Quantum Computer Technology,  
School of Physics, The University of New South Wales, Sydney, Australia*

(Dated: November 3, 2018)

## Abstract

The authors demonstrate readout of electrically detected magnetic resonance at radio frequencies by means of an LCR tank circuit. Applied to a silicon field-effect transistor at milli-kelvin temperatures, this method shows a 25-fold increased signal-to-noise ratio of the conduction band electron spin resonance and a higher operational bandwidth of  $> 300$  kHz compared to the kHz bandwidth of conventional readout techniques. This increase in temporal resolution provides a method for future direct observations of spin dynamics in the electrical device characteristics.

PACS numbers: 03.67.Lx, 72.20.-i, 73.40.Qv, 73.43.Fj

Keywords: silicon, phosphorus, Si, MOSFET, tank circuit, spin, 2DEG, electrically detected magnetic resonance, EDMR, ESR, Si:P, quantum computing, rfEDMR, LCR, resonant circuit

---

<sup>\*</sup>corresponding author huebl@wmi.badw.de; present address: Walther-Meissner-Institut, Bayerische Akademie der Wissenschaften, Garching, Germany

<sup>†</sup>present address: Department of Physics, University of Utah, 115 S 1400 E, Suite 201, Salt Lake City, Utah 84112-0830, USA

<sup>‡</sup>present address: Cavendish Laboratory, JJ Thomson Avenue, Cambridge CB3 0HE, United Kingdom

Spin resonance is commonly used to spectroscopically identify spin species in material systems, particular in semiconductors, [1] and it also allows spin dynamics to be studied using pulsed excitation techniques.[2] Although classical spin resonance has the ultimate detection bandwidth, as the signal is detected directly via the re-emission of microwave radiation, the technique is usually limited to large spin ensembles.[3] In order to investigate few [4] and ultimately a single spin [5, 6, 7, 8] the spin information is transferred to a secondary quantity, such as charges or photons, which can be detected sensitively. Such direct electrical readout in electrically detected magnetic resonance (EDMR) is typically limited to the low bandwidths in the kHz regime. Therefore, coherent spin information can only be recovered from the long term electronic evolution of the sample after the microwave pulse.[9, 10] The development of radio frequency (RF) detection schemes for single-electron transistor (SET) electrometry [11] has overcome the limitation of low bandwidth. This has been achieved by embedding the sample in a resonant LCR circuit, which matches the probed resistance information to the impedance of the rf-circuitry of  $50 \Omega$ , allowing the measurement of the sample resistance at high bandwidths.

In this letter we apply the LCR tank circuit developed for radio frequency SETs to the detection of spin phenomena (in the following referred to as rfEDMR). We measure the RF reflectance of the LCR circuit as well as the low-frequency resistance of a metal-oxide-semiconductor-field-effect-transistor (MOSFET), and observe changes in both quantities under electron spin resonance. Furthermore, the temporal dependence of rfEDMR is studied and compared to conventional (low-frequency) EDMR demonstrating the high bandwidth of rfEDMR. This could in principle allow the direct investigation of coherently manipulated spin states, like Rabi oscillations as opposed to the reconstruction discussed in detail in Ref. [9].

Using a LCR resonant circuit for the detection of EDMR requires that the change in the device resistance, monitored at virtually DC ( $< 10$  kHz), can be detected at the resonance frequency  $f_{RF}$  of the LCR circuit, typically a few hundred MHz. While this seems valid for high device mobilities, e.g. transport in the conduction band of Si,[12] systems where the transport is hopping mediated [13] may be an example where this method is not applicable. For a silicon MOSFET, the spin-to-charge conversion process originates from a difference in scattering amplitudes for randomly formed spin pairs in singlet and triplet configuration in the MOSFET channel, the relative contribution of which is changed under spin resonance

conditions, leading to a change in the total conductance of the electron accumulation layer by  $\Delta\sigma/\sigma \approx 10^{-4}$ . [12, 14, 15] Incorporating this device as the resistive element in a LCR resonant circuit allows us to measure resistance changes via the magnitude of the absorption at  $f_{RF}$ . [11] This is conveniently measured in reflection, where the reflection coefficient  $\Gamma$  is determined by the impedance mismatch between the coaxial line and the LCR circuit. In EDMR spin resonance manifests in a change  $\Delta R$  of the total device resistance  $R$  and for rfEDMR small changes in  $\Delta R$ , close to the matching condition  $|Z_{LCR}(f)| \approx 50 \Omega$ , will result in a change of  $\Gamma \propto \Delta R$ . Additionally, calibration of the RF reflectance can be obtained by measuring the DC device resistance simultaneously and assuming that it is independent of the probe frequency. [11] The resistance can then be accessed quantitatively using the RF circuit, retaining the benefit of the increased bandwidth.

The MOSFET (cf. Fig. 1 (a)) investigated is fabricated on natural bulk silicon with a phosphorus doping of  $[P] = 8 \times 10^{16} \text{ cm}^{-3}$  and has a 20 nm thick, high-quality  $\text{SiO}_2$  gate oxide. Source and drain contacts are formed by indiffused phosphorus regions with  $[P] = 3 \times 10^{19} \text{ cm}^{-3}$ . [14] A shorted strip line is used simultaneously as a gate electrode, to accumulate electrons, and as a local antenna to provide the microwave magnetic field  $B_1$  which excites the spin transitions. The MOSFET is turned on by grounding the gate and applying a differential voltage across the source and drain contacts  $V_{SD}$ , commonly offset from the top gate potential  $V_G$  and the source drain current  $I_{SD}$  is measured by a current amplifier (SIM918). For the experiments shown here, the microwave frequency applied is  $f_{MW} = 37.9044 \text{ GHz}$  with a source power of 10 dBm. In order to employ phase-sensitive detection with a lock-in amplifier we modulate the frequency of the microwave sinusoidally with variable rate  $f_{mod}$  and a depth of 1.5 MHz equivalent to 0.2 mT magnetic field modulation. [14] The experiment is performed in a dilution refrigerator at  $\approx 200 - 300 \text{ mK}$ , which is inserted into a superconducting magnet to provide a static magnetic field  $B_0$ , oriented along the [001]-direction of the Si crystal and perpendicular to the sample surface. Additionally,  $B_0$  is corrected for a constant offset, using the  $^{31}\text{P}$  hyperfine split signature with a center of gravity  $g$ -factor of 1.9985 of a reference spectrum. [16] Figure 1 (a) shows the DC and RF part of the electrical setup used for EDMR detection in this experiment. The LCR circuit is realized by a surface mount inductor ( $L = 330 \text{ nH}$ ) on a printed circuit board located close to the source contact of the MOSFET. The capacitance ( $C \approx 500 \text{ fF}$ ) is given by the parasitic capacitance from source to drain and drain to the gate. The resistor  $R$  is formed by the source-to-drain resistance of the

MOSFET. The resonance frequency of this circuit under matching conditions is 385.13 MHz defining the RF frequency  $f_{RF}$  used for rfEDMR. Additionally,  $C_{in}$  and  $C_{out}$ , each 100 pF, in combination with 1 k $\Omega$  NiCr resistors and 470 nH surface mount inductors form biasing tees, decoupling the RF and DC signals. The RF reflectometry is realized by sending an RF signal to a directional coupler (15 dB, at the 4 K stage) and amplifying the reflected signal with a Quinstar cold amplifier ( $T_N = 3.1$  K) located at the 4 K stage. After demodulating the amplified reflected RF signal using a homodyne detection scheme, involving quadrature demodulation (AD8348) at room temperature, the resulting DC signal  $V_{IF} \propto \Gamma$  is recorded by either a lock-in amplifier or by a digital storage oscilloscope (DSO).

In order to calibrate the RF detection setup, we record the source-drain current  $I_{SD}$  as well as the demodulated RF signal  $V_{IF}$  for  $f_{RF} = 385.13$  MHz as function of the top gate voltage  $V_G$ . Figure 1 (b) shows  $V_{IF}$  as function of  $I_{SD}$  or  $1/R_{SD}$  for a source-drain bias  $V_{SD} = 1$  mV. In the  $I_{SD}$  regime between 6 nA and 30 nA, we observe a linear relation of -57.9 mV/nA, which we use to convert  $V_{IF}$  into  $I_{SD}^{IF}$  and  $\Delta I_{SD}^{IF}$ . The presence of a matching point in the response of the tank circuit is a particular advantage of rfEDMR, because here  $\Gamma \propto \Delta R$  which suppresses the finite  $I_{SD}$  intrinsically. In contrast, conventional EDMR generally suffers from the challenge of measuring a small resistance or current change on a relatively large current offset.

Figure 2 compares the different EDMR detection modes for a gate voltage  $V_g = 0.64$  V, a source-drain bias  $V_{SD} = 1$  mV resulting in  $I_{SD} = 23.4$  nA, close to matching of the LCR circuit. Panel (a) shows the lock-in detected source drain current  $\Delta I_{SD}$  of a conventional EDMR spectrum acquired over a total of 30 magnetic field scans. Two resonant lines are observed, one at  $B_0 = 1.35429$  T corresponding to  $g = 1.9997$  in good agreement with the conduction band electron signal of the accumulation layer [16] and a second one at  $B_0 = 1.35474$  T ( $g = 1.999$ ) possibly originating from exchange coupled P donors.[17] Interestingly, the two hyperfine-split lines expected for isolated phosphorus donors in silicon are not present in this spectrum. Their absence appears to be related to the bias conditions of the MOSFET, as they are present for higher source-drain bias (50 mV) and lower  $V_G$  (0.3 V - not shown). This could be due to the trapping of electrons in a diamagnetic P<sup>-</sup> state which is ESR inactive. This state is approx 2-3 meV below the conduction band and therefore, the thermal excitation at low temperatures  $\propto 200 - 300$  mK and the resulting slow escape rate could explain the absence of the lines,[18] whereas for high bias conditions an

increased escape rate due to tunneling is expected. This effect, whilst interesting, is beyond the scope of this publication focussing on the high-bandwidth readout, and will be discussed elsewhere.

Figure 2 (b) shows the demodulated and lock-in amplified reflected RF signal, converted into an equivalent current using the calibration curve of Fig. 1 (b) measured under the same conditions as in Fig. 2 (a). This spectrum was obtained in a single magnetic field scan with an incident RF power of -55 dBm or  $\sim 0.4$  mV at the input of the LCR circuit, similar to the dc bias applied. Fig 2 (b) shows a significantly better signal-to-noise ratio of  $S/N|_1 = 15$  per field scan in contrast to the conventionally acquired data shown in (a) with  $S/N|_1 = 0.65$  normalized to one scan. The improved signal-to-noise ratio could originate from two effects: (i) at higher probe frequencies in the  $1/f$  regime the noise level of the MOSFET is reduced [19] and (ii) the cold amplifier has a better noise performance than the room temperature current amplifier. This high signal-to-noise ratio enables monitoring the device resistance sensitively enough to observe spin-dependent resistance changes by direct acquisition of  $V_{IF}$  with DSO. Figure 2 (c) shows  $V_{IF}$  converted to  $I_{SD}^{IF}$  using Fig. 1 (b) averaged over 9 magnetic field scans. Each field point consists of the mean value of  $V_{IF}$ , obtained for a 1024-points time trace, where each trace is averaged for 128 times. The ability to directly acquire  $I_{SD}^{IF}$  in the time domain with a precision that allows to resolve spin-dependent features is the prerequisite for investigating dynamic effects, e.g. resistance changes during or after microwave pulses. In general, the detection bandwidth is limited by the quality factor of the LCR circuit, in this case 20 MHz. This would technically allow the direct monitoring of Rabi oscillations, since a typical Rabi frequency in pulsed ESR/EDMR spectrometers is 5-20 MHz [9] and should be 2.8 MHz in the devices used in these experiments, based on  $B_1 = 0.1$  mT obtained from numerical modeling.[14]

To experimentally explore the bandwidth of rfEDMR, we investigate the spin-resonant resistance change as function of the microwave frequency modulation rate  $f_{mod}$ . Figure 3 compares the conventionally measured (lock-in amplified) peak-to-peak signal amplitudes obtained for the conduction band electron signal at  $B_0=1.35429$  T (blue squares) to the data acquired via the reflected RF signal in the tank circuit, again lock-in amplified (solid black circles). While the conventionally detected signal shows a 3 dB compression at  $f_{mod} \approx 15$  kHz, as expected for a device resistance of  $\approx 30$  k $\Omega$  and cable capacitance of  $C_{cable} \approx 400$  pF resulting in a  $f_{RC} \approx 13$  kHz, the  $\Delta I_{SD}^{IF}$  obtained via the lock-in amplifier shows

no frequency dependence up to 100 kHz, the maximum frequency of the SR830 lock-in amplifier. To extend the accessible frequency beyond this limitation, we directly digitized  $V_{IF}$  using a DSO and calculate the lock-in signal numerically (solid black circles). For the digital data acquisition we kept the number of recorded modulation periods constant. The response of the LCR circuit measured with the SR830 and the 'numerical lock-in data' agree quantitatively in the overlapping range, resulting in a measured  $f_{3dB} \approx 300$  kHz. This limit is attributed to the SR560 voltage preamplifiers used to post-amplify the output of the quadrature demodulation board and could be overcome by higher bandwidth preamplifiers.

In conclusion, we present a high bandwidth detection method to observe EDMR using a LCR tank circuit. Measuring rfEDMR for a silicon MOSFET, quantitative agreement with conventionally detected EDMR is demonstrated with a 25-fold increase in the signal-to-noise ratio and a detection bandwidth  $> 300$  kHz. These two properties are the key requirement to probe dynamic spin information in the conductance directly, e.g. Rabi oscillations during ESR pulses. Finally, this technique should be sensitive to capacitive changes in the LCR circuit as well and might be applicable to capacitive detected magnetic resonance studies.[20]

The authors thank D. Barber for technical support in the National Magnet Laboratory at UNSW. This work is supported by the Australian Research Council, the Australian Government, and by the U.S. National Security Agency (NSA) and U.S. Army Research Office (ARO) (under Contract No. W911NF-04-1-0290).

- 
- [1] J.-M. Spaeth and H. Overhof, *Point defects in Semiconductors and Insulators* (Springer, Berlin, 2003).
  - [2] A. Schweiger and G. Jeschke, *Principles of Pulse Electron Paramagnetic Resonance* (Oxford University Press, New York, 2001).
  - [3] D. C. Maier, Bruker Rep. **144**, 13 (1997).
  - [4] D. R. McCamey, et al., Appl. Phys. Lett. **89**, 182115 (2006).
  - [5] L. Childress, et al., Science **314**, 281 (2006).
  - [6] F. H. L. Koppens, et al., Nature **442**, 776 (2006).
  - [7] J. Wrachtrup, et al., Nature **363**, 244 (1993).
  - [8] J. Köhler, et al., Nature **363**, 242 (1993).

- [9] A. R. Stegner, et al., *Nature Phys.* **2**, 835 (2006).
- [10] H. Huebl, et al., *Phys. Rev. Lett.* **100**, 177602 (2008).
- [11] R. J. Schoelkopf, et al., *Science* **280**, 1238 (1998).
- [12] C. F. O. Graeff, et al., *Phys. Rev. B* **59**, 13242 (1999).
- [13] M. Stutzmann, M. S. Brandt, and M. W. Bayerl, *Journal of Non-Crystalline Solids* **266-269**, 1 (2000).
- [14] L. H. Willems van Beveren, et al., *Appl. Phys. Lett.* **93**, 072102 (2008).
- [15] R. N. Ghosh and R. H. Silsbee, *Phys. Rev. B* **46**, 12508 (1992).
- [16] C. F. Young, et al. *Phys. Rev. B* **55**, 16245 (1997).
- [17] P. R. Cullis and J. R. Marko, *Phys. Rev. B* **11**, 4184 (1975).
- [18] G. W. Morley, et al. *Phys. Rev. Lett.* **101**, 207602 (2008).
- [19] R. Sarpeshkar, T. Delbrück, and C. Mead, *IEEE Circuits and Devices* **9**, 23 (1993).
- [20] M. S. Brandt, R. T. Neuberger, and M. Stutzmann, *Appl. Phys. Lett.* **76**, 1467 (2000).

## Figures

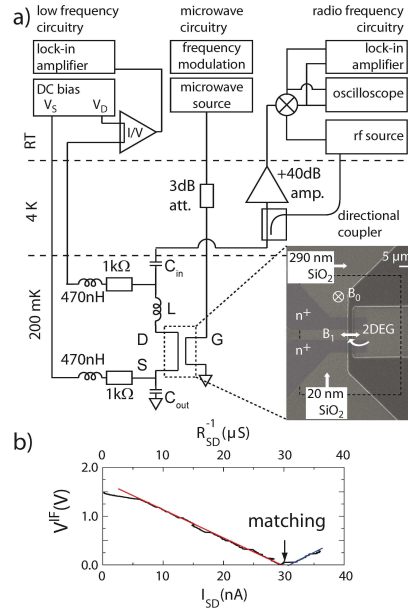


FIG. 1: (color online) Panel (a) shows the EDMR detection setup including the low frequency, the microwave, and the radio-frequency circuitry. The inset shows a scanning electron micrograph of the silicon MOSFET. Panel (b) shows the calibration curve that translates the source-drain conductance/current ( $V_{SD} = 1$  mV) to the reflected RF signal amplitude after homodyning  $V_{IF}$ . At 30 nA a matching point is observed. The red and blue lines are guides to the eye and show a slope of -57.9 mV/nA and 48 mV/nA, respectively.

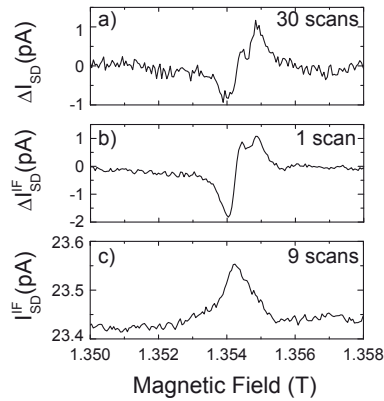




FIG. 2: EDMR using different detection schemes. Panel (a) shows the EDMR signal obtained by monitoring the lock-in amplified source drain current. Panel (b) shows the reflected RF signal from the LCR circuit using homodyne detection, lock-in amplification, and conversion to a current scale using Fig. 1 (b) with a 25-fold increased signal-to-noise. Panel (c) shows the absolute (converted) current change, monitored directly by measuring  $V_{IF}$  with a storage oscilloscope.

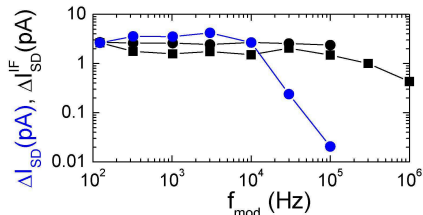


FIG. 3: Frequency modulation rate dependence of the signal amplitudes for conventional EDMR and rfEDMR detection. The blue circles represent the peak-to-peak amplitude of the conduction band electron ESR signal using conventional EDMR, decreasing at  $\approx 15$  kHz. The rfEDMR lock-in signal (black circles) matches the conventional EDMR data up to  $f_{mod} \approx 15$  kHz and shows no decrease up to 100 kHz. Using a digital storage oscilloscope  $I_{SD}^{IF}$  was recorded up to  $f_{mod} = 1$  MHz and the lock-in response determined numerically (black squares). Here, the signal amplitude starts to drop at about 300 kHz, attributed to the voltage preamplifiers used.